# Frequency-Dependent Characteristics of Open Microstrip Lines with Finite Strip Thickness

CHIN SHIH, RUEY-BEEI WU, SHYH-KANG JENG, MEMBER, IEEE, AND CHUN HSIUNG CHEN

*Abstract*—**A rigorous approach based on the variational conformal mapping technique is proposed for analyzing the characteristics of open microstrip lines with finite strip thickness. By Chang's mapping, the solution domain becomes a finite and nearly rectangular region in which the finite element method is applied. The wedge conditions at the strip corners, which are very difficult to discuss by the conventional methods, are now correctly handled. Numerical results included here are the current distributions around the strip and variations of the effective dielectric constant caused by the finite-thickness effect.**

## I. Introduction

The finite-thickness effect of microstrip lines plays an important role in microwave integrated circuits [1], [2]. Typically, the strip thickness is 1–3 $\mu$m in monolithic microwave integrated circuits and 5–20 $\mu$m in hybrid microwave integrated circuits [3].

Based on the quasi-TEM approach, several methods have been proposed to calculate the capacitance of microstrip lines [4]–[6]. Among them, the conformal mapping technique is simple and useful. Wheeler [5] introduced an elementary mapping function to get the results when the thickness of the strip is negligible. Chang derived another mapping to take the effect of the thickness into account [6].

Concerning the full-wave analysis, the spectral-domain approach [7] was proposed to study the characteristics of a dispersive microstrip line. With the conventional finite element method [8], one would encounter difficulty in handling the fields around the strip corners. Recently, Bogelsack [9] has tried the mode-matching technique together with the projection method to analyze the characteristics of a closed microstrip line with finite strip thickness. Some empirical expressions [10] are also available for finite-thickness microstrips.

In this paper, the effect of the strip thickness on the characteristics of the open microstrip line is determined by the variational conformal mapping technique [11]. By employing Chang's mapping [6], not only is the original infinite domain simplified into a nearly rectangular region, but also the field singularities around the strip corners are well treated. This makes our numerical analysis more meaningful. Numerical results, including the effective dielectric constant and the strip current distributions, are presented.

## II. Variational Conformal Mapping Technique

Shown in Fig. 1 is a typical open microstrip line which has a strip of width $w$ and a thickness of $t$, while the dielectric underneath has height $h$ and relative permittivity $\epsilon_r$. By symmetry with respect to the $y-z$ plane, we need only consider the half structure with $x \geq 0$, shown in Fig. 2(a). As far as the lowest ($E_z$ even and $H_z$ odd) mode is concerned, we may equivalently place a magnetic wall at the plane $x = 0$.

Manuscript received March 22, 1988; revised November 7, 1988. This work was supported by the National Science Council, Republic of China, under Grant NSC 76-0404-E002-13.

The authors are with the Department of Electrical Engineering, National Taiwan University, Taipei 10764, Taiwan, Republic of China.

IEEE Log Number 8826057.

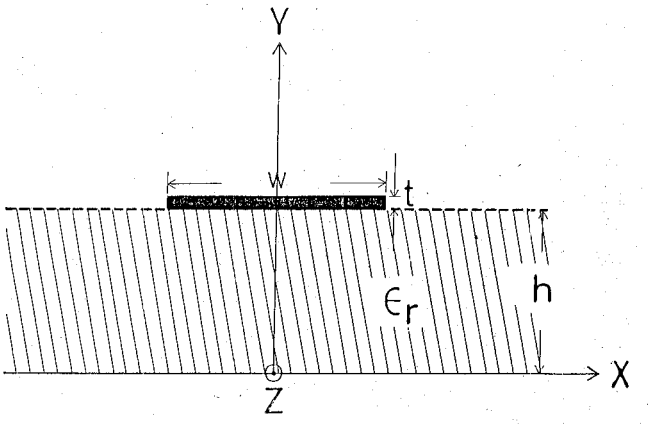


Fig. 1. Geometry of microstrip line with finite strip thickness.

By choosing a suitable mapping function to transform the original infinite domain into a suitable finite image domain, the variational conformal mapping technique achieves an $(E_z, H_z)$ variational formulation in the image domain [11, eq. (7)]. Then the propagation constant and the fields can be solved in the image domain by the finite element method [11]. For microstrip lines with finite strip thickness, an appropriate choice is Chang's mapping [6], which transforms the original $z$ $(= x + iy)$ domain (Fig. 2(a)) into the image $z'$ $(= x' + iy')$ domain (Fig. 2(b)). The desired mapping function and the Jacobian are

$$z - w/2 = \frac{\pi}{h}\left[\left(\frac{p+1}{p^{1/2}}\right)\tanh^{-1} R + \left(\frac{p-1}{p^{1/2}}\right)\left(\frac{R}{1-R^2}\right) + \ln\left(\frac{Rp^{1/2}-1}{Rp^{1/2}+1}\right)\right]$$

$$J = \left|\left[\frac{h(V+1)^{1/2}(V+p)^{1/2}}{p^{1/2}V}\right] \cdot \left\{\frac{d\exp(\pi z')(a-1)(a+b+1)^2}{[(a+b)-(1+b)\exp(\pi z')]}\right\}\right|^2$$

where

$$R = \left(\frac{V+1}{V+p}\right)^{1/2}$$

$$V = \frac{ad\exp(\pi z') - d}{[(a+b)-(1+b)\exp(\pi z')]}.$$

The parameters $a$, $b$, $d$, and $p$ are determined by the thickness $t$, the width $w$, and the height $h$ [6]. Since the image domain is nearly rectangular, the mesh division for finite element analysis may easily be achieved in the image domain. Also shown in Fig. 2(a) and (b) are typical mesh divisions in both original and image domains. It should be noted that the mapping cannot handle the case of $t = 0$.

As described in [11, eqs. (8) and (9)], the transverse fields in the original domain can be obtained from the Jacobian and the virtual fields in the image domain. In addition, the singularities associated with the transverse fields can be circumvented if the mapping is chosen such that the virtual fields are smooth and finite all over the image domain. For this problem, the transverse

0018-9480/89/0400-0793$01.00 ©1989 IEEE

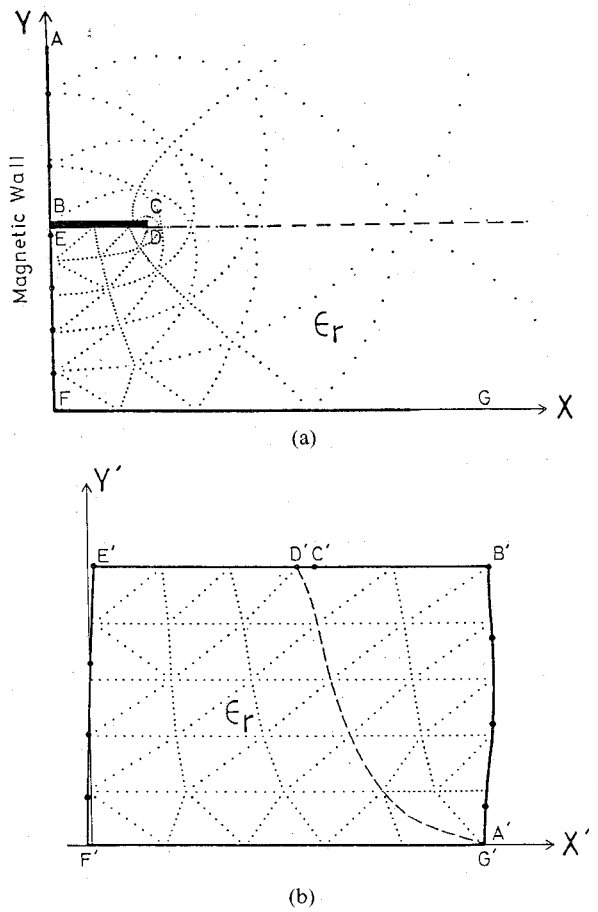


Fig. 2. Mesh divisions in (a) original domain and (b) image domain. Mesh numbers = 5×5.

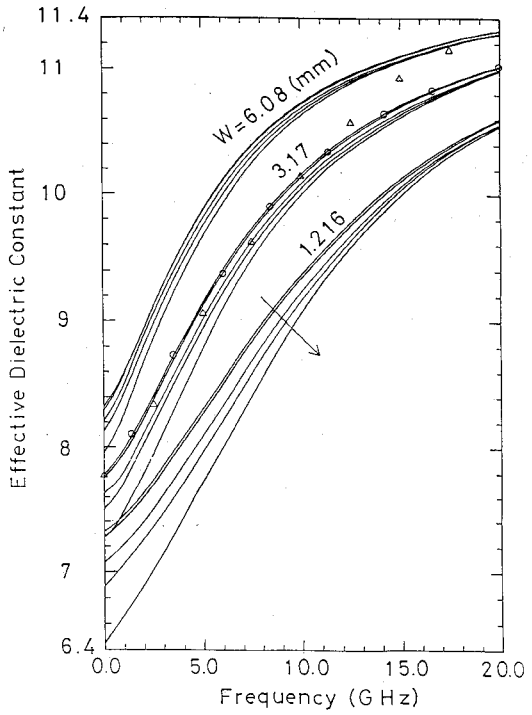


Fig. 3. Effective dielectric constant versus frequency ($h = 3.04$ mm, $w = 1.216$, 3.17, 6.08 mm, $t = 0.0001, 0.01, 0.1, 0.2, 0.5$ mm, $\epsilon_r = 11.7$). ○○○○ Shih [11]; △△△△ Itoh [7]; ——— present method. The arrow indicates the increase of $t$.

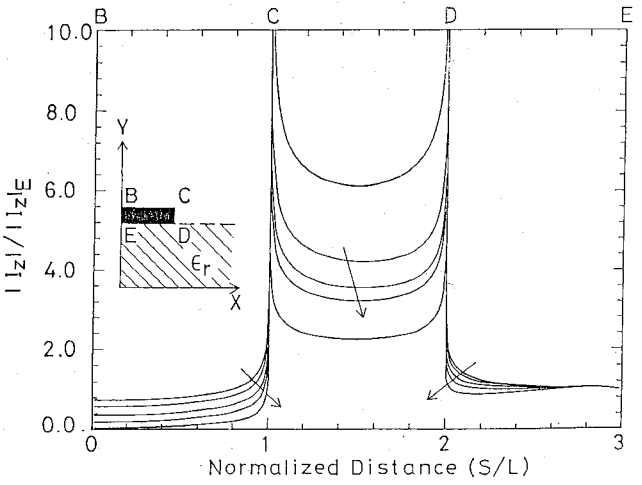


(a)

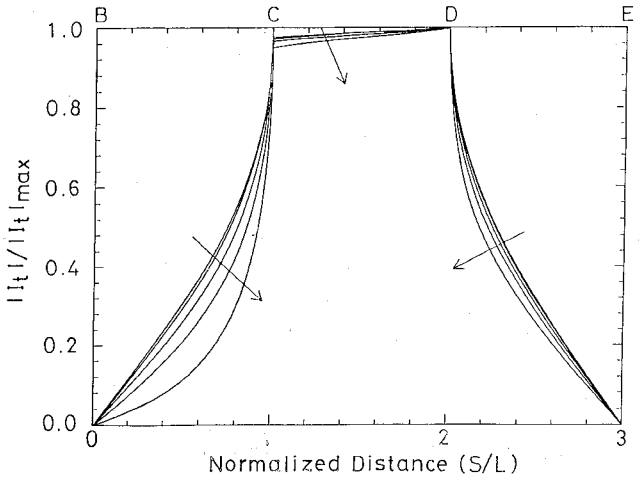


(b)

Fig. 4. Normalized strip current distributions versus normalized distance with frequencies as parameters ($h = 3.04$ mm, $w = 3.17$ mm, $t = 0.001$ mm, $\epsilon_r = 11.7$, frequency $= 1, 3, 6, 10, 20$ GHz). The symbols $L$ and $S$ denote the length and the distance of each contour, where $S$ is measured in clockwise fashion along the strip. $|I_z|_E$ is the longitudinal current at the point $E$ and the arrows indicate the increase of frequency. (a) Longitudinal and (b) transverse current distributions.

fields near the strip corner are proportional to $r^{-1/3}$, where $r\ (=\sqrt{x^2+y^2})$ is the distance from the corner. It is not difficult to verify that $\sqrt{J}$ tends to $r^{1/3}$ near the corners. Therefore, the wedge conditions are correctly handled and the virtual fields are smooth and finite all over the image domain.

## III. Numerical Results and Discussions

### A. Effective Dielectric Constant

The effective dielectric constants (as defined by [11, eq. (6)]) for several structures are shown in Fig. 3. Our results as $t$ tends to 0 are in good agreement with Shih's [11]. Both can be compared with Itoh's [7], which neglect the thickness of the strip. As with the empirical expressions [2], there appears to be only a slight finite-thickness effect on our numerical results for typical structures employed in the practical design where the strip thickness is smaller than 20 $\mu$m. However, it is found that the divergence becomes clearer as the value of $t$ increases.

The finite-thickness effect is also found to be less significant at higher frequencies than at lower frequencies. This implies that the power is more densely confined to the dielectric under the strip as the frequency increases. Hence, the thickness of the strip has a smaller effect at higher frequencies. This inference will be made clear when the current distributions along the strip are presented.

### B. Current Distributions

From the transverse magnetic field, the current density along the strip can be found. The longitudinal current distributions ($|I_z|/|I_z|_E$) around the strip are shown in Fig. 4(a). It is found that the currents along the $D-E$ contour become more dominant than those along the others as the frequency increases. That is, the higher the frequency, the more the transverse fields are confined to the substrate below the strip. This reflects the fact that the effective dielectric constant eventually tends to the dielectric constant of the substrate.

For the same cases as above, the transverse current distributions ($|I_t|/|I_t|_{\max}$) are shown in Fig. 4(b). On the whole, the increase in frequencies causes greater variations to the current distributions along the $B-C$ contour than those along the $C-D$ and $D-E$ contours. Especially at the higher frequency, the difference between the distributions at the corners $C$ and $D$ becomes more pronounced. In other words, the transverse current concentrates mainly near the corner $D$ as the frequency increases.

## IV. Conclusions

A full-wave analysis based on the variational conformal mapping technique to analyze the open microstrip line with finite strip thickness has been presented. Chang's mapping makes numerical analysis feasible. Numerical results are presented and are consistent with available data. The results provide the effective dielectric constants for the thicker strip. The numerical results also disclose that the longitudinal current distributions around the strip are confined to the substrate below the strip and that the transverse current distributions concentrate mainly toward the corner $D$ as the frequency increases.

## References


[1] R. A. Pucel, *Monolithic Microwave Integrated Circuits*. New York: IEEE, 1985.

[2] K. C. Gupta, R. Garg, and I. J. Bahl, *Microstrip Lines and Slotlines*. Dedham, MA: Artech House, 1979.

[3] P. Waldow and I. Wolff, "The skin-effect at high frequencies," *IEEE Trans. Microwave Theory Tech.*, vol. MTT-33, pp. 1076–1082, Oct. 1985.

[4] E. Yamashita and R. Mittra, "Variational method for the analysis of microstrip lines," *IEEE Trans. Microwave Theory Tech.*, vol. MTT-16, pp. 251–256, Apr. 1968.

[5] H. A. Wheeler, "Transmission line properties of parallel strip separated by a dielectric sheet," *IEEE Trans. Microwave Theory Tech.*, vol. MTT-13, pp. 172–185, Mar 1965.

[6] W. H. Chang, "Analytical IC metal-line capacitance formulas," *IEEE Trans. Microwave Theory Tech.*, vol. MTT-24, pp. 608–611, Sept. 1976.

[7] T. Itoh and R. Mittra, "Spectral-domain approach for calculating the dispersion characteristics of microstrip lines," *IEEE Trans. Microwave Theory Tech.*, vol. MTT-21, pp. 496–498, July 1973.

[8] P. Daly, "Hybrid-mode analysis of microstrip by finite-element methods," *IEEE Trans. Microwave Theory Tech.*, vol. MTT-19, pp. 19–25, Jan. 1971.

[9] F. Bogelsack and I. Wolff, "Application of projection method to a mode-matching solution for microstrip lines with finite metallization thickness," *IEEE Trans Microwave Theory Tech.*, vol. MTT-35, pp. 918–921, Oct. 1987.

[10] T. C. Edwards, *Foundations for Microstrip Circuits Design*. New York: Wiley, 1981

[11] C. Shih, R. B Wu, S. K. Jeng, and C. H. Chen, "A full-wave analysis of microstrip lines by variational conformal mapping technique," *IEEE Trans. Microwave Theory Tech.*, vol. 36, pp. 576–581, Mar 1988.


# An Improved Design of Systems Based on Three Coupled Microstrip Lines

NABIL A. EL-DEEB, SENIOR MEMBER, IEEE

***Abstract*—An improved design of systems based on three coupled microstrip lines is introduced. The improvement lies mainly in the use of equal-mode-impedance lines, which greatly facilitates the design of the system. The design parameters of such a system are introduced in a manner that allows a simple systematic design procedure. An experimental coupler is realized and its practical performance is in good agreement with the theory.**

## I. Introduction

The use of multiple coupled line structures, including three-line structures, for various applications in communications and microwave engineering has been extensively studied in the literature (e.g. [1]–[10]). The majority of these studies concentrated on the analysis of three-line systems and few considered the design parameters. A general three-line system, where the three lines have different widths and separations, is the most difficult to design and therefore only its analysis is considered (e.g. [8]). Meanwhile symmetrical three-line systems are found to be interesting in several applications (e.g. [1], [4], [5], [6]). Three equal-width coupled lines ($W_2 = W_1$, Fig. 1) are found to have five modal impedances, four of which are independent [9]. The line impedance for a given mode can be defined as the ratio of the voltage on a line to ground divided by the line current when the lines are propagating that mode. If the impedances of the three lines are equal when considering each mode separately there will be only three modal impedances and the system can be called an equal-mode-impedance system. This greatly facilitates the design of three-line systems. The equality of mode impedances is achieved by an appropriate increase of the width of the middle line ($W_2$) relative to that of the outer lines ($W_1$, see Fig. 1). The ratio ($W_2/W_1$) to achieve this equality has been determined for various combinations of geometrical dimensions of the three-line system on an alumina substrate ($\epsilon_r = 9.8$) [9].

In this paper the design parameters for a system of equal-mode-impedance lines are introduced in a manner that allow a simple systematic design of components. The design procedure is illustrated by designing a coupler to satisfy certain conditions, and the results agree well with the theory. Although the substrate material being considered is alumina, the procedure is applicable to other substrate materials (e.g. Teflon ($\epsilon_r = 2.2$) and quartz ($\epsilon_r = 3.78$)).

Manuscript received April 29, 1988; revised November 18, 1988
The author is with the Department of Electrical Engineering, Military Tech. College, Cairo, Egypt.
IEEE Log Number 8826055.